NUMERICAL STUDY OF UNSTEADY BREAKING WAVES INDUCED BY A SUBMERGED HYDROFOIL AT STEADY FORWARD…

Conference Paper · June 2015

4 authors:

Giorgio Contento
Università degli Studi di Trieste
29 PUBLICATIONS   **147** CITATIONS

SEE PROFILE

Guido Lupieri
Università degli Studi di Trieste
14 PUBLICATIONS   **8** CITATIONS

SEE PROFILE

Hrvoje Jasak
University of Zagreb
121 PUBLICATIONS   **2,458** CITATIONS

SEE PROFILE

Vuko Vukcevic
University of Zagreb
17 PUBLICATIONS   **10** CITATIONS

SEE PROFILE

Some of the authors of this publication are also working on these related projects:

Project   Numerical Modelling of Coupled Potential and Viscous Flow for Marine Applications View project

Project   Bachelor thesis project View project

NUMERICAL STUDY OF UNSTEADY BREAKING WAVES INDUCED BY A SUBMERGED HYDROFOIL AT STEADY FORWARD SPEED

Giorgio Contento[1], Guido Lupieri[1], Hrvoje Jasak[2, 3], Vuko Vukčević[2]

[1] HyMO*Lab* - Department of Engineering and Architecture - University of Trieste, Italy

[2] Faculty of Mechanical Engineering and Naval Architecture - University of Zagreb, Croatia

[3] Wikki Ltd., Unit 459 Southbank House, United Kingdom

ABSTRACT

In this work we analyse the features of the unsteady breaking of two dimensional free surface waves induced by a submerged hydrofoil at steady forward speed. The study is conducted by means of numerical simulations with OpenFOAM: `interFoam` and `swenseFoam` solvers being used as a computational framework for the free-surface treatment with the Volume Of Fluid (VOF) and Level Set (LS) techniques respectively. Due to the strongly unsteady behaviour of the flow, the interest is here focused on the spectral content of the free surface elevation. The results from two interface-capturing methods, VOF and LS are discussed and compared with experimental data from the literature. The influence of the turbulence models on the free surface shape and spectral content is also discussed. The final goal of the entire research work is the simulation of complex two-phase flows for robust and fast engineering applications in the ship hydrodynamics and wave loads fields, including wave breaking phenomena.

Giorgio Contento, Guido Lupieri, Hrvoje Jasak, Vuko Vukčević

1 INTRODUCTION

The study of waves and in particular that of breaking waves is important in Naval Architecture and Marine Engineering. It strongly relates to the ship resistance in steady and unsteady flow, therefore the results can provide useful informations for the design of new and more efficient hulls. The appearance of a breaker at the bow relates to a trough of the following wave train and to the inception of a turbulent shear under the free surface. These effects have been experimentally studied by Dong et al. (1997) and Roth et al. (1999), but despite the important changes that a breaking wave induces on the flow around the hull, the presence of a breaker can still lack an accurate reproduction with numerical instruments.

In the context of the RANSE approach, the phenomenon of breaking waves can be parameterized as in Muscari and Mascio (2004) when it is not possible to reproduce it effectively since the full scale Reynolds and Froude number simulations are still challenging to afford for viscous calculation of the entire ship hull. This has fed the interest in the studies of air-water interface conducted with laboratory measurements, starting for instance from Duncan (1981, 1983, 2001).

The study of breaking waves induced at the air-water interface by a submerged obstacle in Blasi et al. (2000), and here numerically reproduced in 2-D simulations, can be considered as a starting point for understanding, handling or calibrating the capabilities of a new solver concerning the dynamics of interface problems, see for instance Lupieri et al. (2012).

In particular, the goal of this paper is to pursue a satisfactory reproduction of the following characteristics of the flow: free surface elevation, wave breaking and low frequency periodicity eventually induced at the wave crest. The paper is organized as follows: the formulation of the problem is described in Sec. 2; the mathematical model for the two phase flow is described in Sec. 3 and the numerical approach is described in Sec. 4. Results are presented and discussed in Sec. 5.

2 PROBLEM FORMULATION

With reference to Fig. 1, the original experimental set-up of Blasi et al. (2000) consists of a NACA-0012 profile foil with chord length $C = 0.4$m submerged with $d/C = 0.65$ in a water channel exposed to a given flux with a horizontal velocity profile $U(y)$ and with angle of attack of $\alpha = 5°$. Similar experiments have been conducted by Duncan (1981, 1983) by towing the submerged foil. Blasi et al. (2000) have originally repeated some of the experiments of Duncan in a circulating channel, measuring the free surface elevation and the flow field by LDV at a slightly higher Reynolds number. Even in steady flow and non breaking conditions with depth of submergence of $d/C = 1.034$, they could not reproduce the longitudinal position of the wave train as measured by Duncan. The differences in the position of the zero-crossings were of order of more than half chord length. The height of the first two waves of the measured train was rather different too. The authors assess these differences as related mainly to the free surface boundary layer induced by the circulating channel at the inlet section, i.e. a non-uniform incident flow. Furthermore, they have shown that the smaller incident speed in the free surface boundary layer acts as a trigger for the breaking, inducing large differences in the longitudinal position of the wave train and in the wave height.

In this paper, we refer to the case with depth $d/C = 0.65$ analyzed by (Blasi et al., 2000) in which a complex foamy free surface has been produced from the spilling breaking effect. In this case, the Froude and Reynolds numbers are respectively $Fr = 0.568$ and $Re = 4.5 \times 10^5$.

The domain for numerical simulations is divided into structured blocks allowing refinements in the near wall region and across the free surface. Close up of the near wall mesh regions for the grid is presented in Fig. 2 (a) and (b).

A convergence analysis has been carried out by refining the grid both in the near wall region of the hydrofoil and in the outer layer. The first grid node at the wall lies at $y^+ \approx 1$, making the turbulence modelling questionable because the laminar sublayer is expected in this region. However, the zone of interest lies at the free surface, far from the hydrofoil. The origin of the Cartesian coordinate system is

located at the leading edge of the hydrofoil; the domain extends $40C$ in downstream and $20C$ upstream of the foil. Distance from the bottom is fixed at $h = 2.25$m. The results shown here refer to a grid with approx. 200,000 cells.

The boundary initial conditions consist of an unperturbed free surface elevation and a steady free stream velocity field assigned at the inlet as in Blasi et al. (2000) with a zero normal derivative for the pressure. A constant total pressure is assigned at the top boundary and the inlet/outlet boundary condition is specified for the velocity field depending on the flow direction. At the outlet, zero normal derivatives are imposed for both velocity and pressure. No slip boundary condition is imposed at the hydrofoil wall.

Simulations with a turbulence model have been carried out with turbulent intensity $I = 10^{-5}$ and eddy viscosity ratio $\beta = \nu_t / \nu = 2 \times 10^2$.
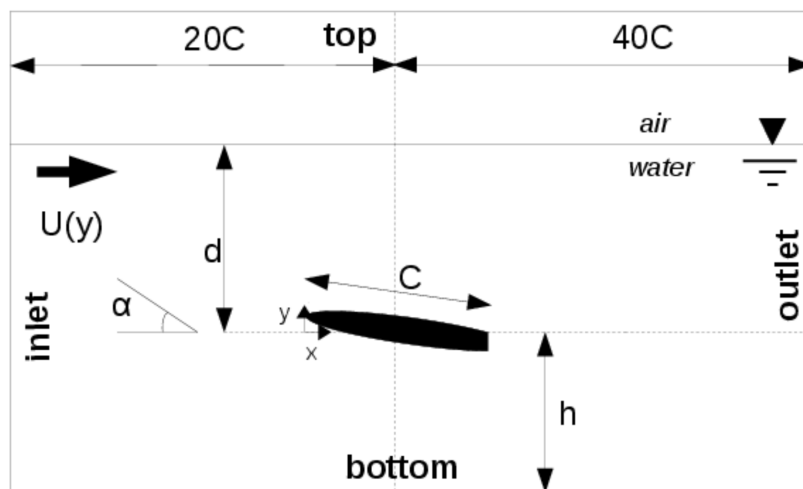

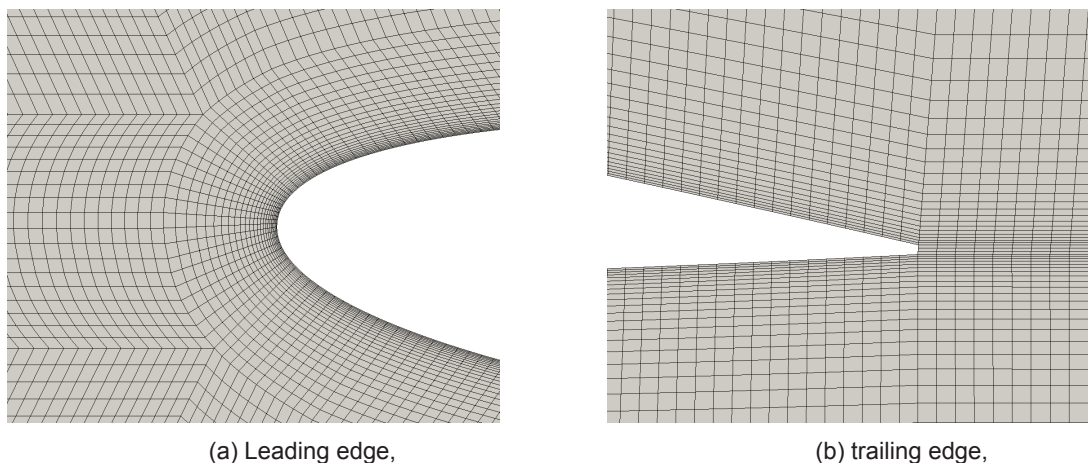Figure 1: Set up of the numerical experiment.

(a) Leading edge,   (b) trailing edge,

Figure 2: Sketches of the computational grid around the leading (a) and trailing (b) edge of the submerged foil.

3   MATHEMATICAL MODEL

The governing equations for an incompressible Newtonian fluid are the momentum and the mass conservation equation:

$$\frac{\partial(\rho u_i)}{\partial t} + \frac{\partial(\rho u_j u_i)}{\partial x_j} = -\frac{\partial p}{\partial x_i} + \frac{\partial}{\partial x_j}\left(\mu\left(\frac{\partial u_i}{\partial x_j} + \frac{\partial u_j}{\partial x_i}\right)\right) + F_i, \tag{1}$$

$$\frac{\partial u_i}{\partial x_i} = 0, \tag{2}$$

where ρ is the fluid density, u_i the velocity field, p the pressure, μ the dynamic viscosity, F_i the buoyancy contribution to the momentum balance, t and x_i the time and spatial independent variables.

For small Reynolds numbers, the Navier-Stokes equations can be solved without any turbulence modelling. When this modelling becomes necessary, an approach based on the reformulation of equations (1) and (2) in terms of Reynolds averaged variables can be obtained. Then, to achieve the closure of the new set of obtained equations, it is possible to add additional equations in order to redefine eddy viscosity. The turbulence model adopted in this study is the $k-\omega$ Shear Stress Transport introduced by Menter (1994) which consists of two additional transport equations: one for the turbulent kinetic energy k and other for a specific turbulence dissipation ω that is directly related to dissipation and turbulent kinetic energy. These two equations are used to update the eddy viscosity appearing in the diffusion term in equation (1).

Being interested in two phase flows (a coupled air-water interface system), we introduce Volume of Fluid (VOF) by Hirt and Nichols (1981) and implicitly redistanced Level Set (LS) interface capturing method by Vukčević et al. (2015), derived from Phase Field equation by Sun and Beckermann (2007). The idea behind VOF is to use a scalar indicator function α to represent the phase of the fluid in each cell. Viscosity and density in Navier-Stokes equations (1) read:

$$\mu = \mu_{water}\alpha + \mu_{air}(1-\alpha), \tag{3}$$

$$\rho = \rho_{water}\alpha + \rho_{air}(1-\alpha), \tag{4}$$

and the α transport equation reads:

$$\frac{\partial\alpha}{\partial t} + \frac{\partial(u_i\alpha)}{\partial x_i} = 0. \tag{5}$$

The α is bounded between 1 (if only water is present in a control volume) and 0 (if only air is present) over an infinitesimal thickness. This leads to numerical difficulties associated with the discretization of the convection term in the equation (5). This in turn results in smearing of the interface. Following (Rusche, 2002), we use a modified transport equation with an additional convective term that serves to compress the interface:

$$\frac{\partial\alpha}{\partial t} + \frac{\partial(u_i\alpha)}{\partial x_i} + \frac{\partial(w_i\alpha)}{\partial x_i} = 0, \tag{6}$$

where w_i is an artificial velocity field that is directed normal to and towards the interface. The relative magnitude of the artificial velocity is determined with the following expression:

$$w_i = K_c n_i^* \max\frac{|n_i^* F|}{|S_i|}, \tag{7}$$

where K_c is an adjustable coefficient that determines the magnitude of the compression, n_i^* is the interface unit normal vector, F is the flux and S_i is the surface area vector.

An alternative way of capturing interface is the LS method by Osher and Sethian (1988) based on signed distance function. The signed distance function is defined positive in water and negative in air,

while the magnitude is obtained as a shortest distance to the interface. Hence, interface location is obtained with the zero level set, $\phi(x_i, t) = 0$. The LS is defined as:

$$\phi(x_i) = \begin{cases} d, & \text{if } x_i \in \Omega_{water}, \\ 0, & \text{if } x_i \in \Gamma, \\ -d, & \text{if } x_i \in \Omega_{air}, \end{cases} \tag{8}$$

where d is the shortest distance to the interface and Γ is the interface. Ω_{water} and Ω_{air} are regions occupied with water and air, respectively.

If the usual convection equation is used to transport the LS field, there is no guarantee that the LS will remain signed distance function. A number of redistancing algorithms exists in literature (Gomez et al., 2005; Hartmann et al., 2008). They are usually based on direct calculation of the distance to the interface after convection or on the introduction of additional redistancing equation. Here, we take a different approach based on Phase Field equation introduced by Sun and Beckermann (2007). With this approach, the LS field remains a signed distance function during the solution process. The LS transport equation reads:

$$\frac{\partial \phi}{\partial t} + \frac{\partial (u_i \phi)}{\partial x_i} = b \left(\frac{\partial \phi}{\partial x_i \partial x_i} + \frac{\sqrt{2}}{\epsilon} \left(1 - \left| \frac{\partial \phi}{\partial x_i} \right|^2 \right) \tanh \left(\frac{\phi}{\epsilon \sqrt{2}} \right) - \left| \frac{\partial \phi}{\partial x_i} \right| \frac{\partial}{\partial x_i} \left(\frac{\frac{\partial \phi}{\partial x_i}}{\left| \frac{\partial \phi}{\partial x_i} \right|} \right) \right). \tag{9}$$

The terms on the right hand side of equation (9) serve to smooth over possible singularities and to preserve the signed distance function during the transport. Reader is referred to (Sun and Beckermann, 2007) for more details.

These equations complete the mathematical formulation of the two phase flow model.

4   NUMERICAL METHOD

LS and VOF methods are implemented in foam-extend (2014) and *OpenFOAM* (2012), hereafter indicated as F-E and O-F respectively. Within these Finite Volume libraries, the solvers used in this study are `swenseFoam` and `interFoam` that include previously defined LS and VOF methods for interface capturing.

Standard $k - \omega$ SST turbulence model by Menter (1994) is adopted for O-F, whereas in the case of F-E, the same turbulence model is used with an eddy viscosity limiter. They are both considered in this study and are indicated as O-Ft and F-Et respectively.

The Navier-Stokes equations are solved over a set of finite control volumes using schemes based on a 2nd order Gaussian integration. Evaluation of the gradient is obtained by linear cell to face interpolation. The Laplacian terms are also evaluated with linear interpolation with non--orthogonal correction. The convection term for the momentum equation is discretized using limited linear interpolation. For the VOF approach, velocity convection term is discretized using Total Variation Diminishing scheme with Van Leer limiter, while the compressive convection term is discretized using an interface compression scheme. The convection term in the LS approach is discretized using the blended scheme with a blending factor of 0.75.

The pressure-velocity coupling is achieved using the PISO algorithm. Euler scheme is adopted to march forward in time. The free-surface location in VOF is computed using the multidimensional universal limiter for explicit solution (MULES). The LS transport equation is discretized and solved implicitly. The details of the discretization are beyond the scope of this paper. Nevertheless, some details about the numerical model can be found in the OpenFOAM user guide (*OpenFOAM*, 2012).

5   RESULTS AND DISCUSSION

The main goal of this study is to resolve the Navier-Stokes equations also in Reynolds Averages formulation to extract information related to breaking wave events.

The approach pursued in this work is twofold: first, the time-averaged free surface shape obtained from the numerical simulations is analyzed following theoretical results after Duncan (1981) and experimental data by Blasi et al. (2000); second, the time varying free surface elevation is analyzed following theoretical results again after Duncan (1981) and experimental data by Blasi et al. (2000).

In the following we give a short recap of some theoretical elements of interest related to the breaker's characteristics, as reported by (Duncan, 1981). Fig. 3 summarizes the main parameters of the recirculating aerated water in the breaker zone. These parameters are: the height a_b and the length λ_b of the breaking wave, the length L, the area A and the angle θ of the breaking region, T_b the period of oscillation; $L sin\theta$ is the vertical component of the length of the breaking region, a and λ are the height and length of the first wave after the first crest.

A relationship between breaking wavelength and incident flow speed in terms of the finite amplitude Stokes wave equation reads:

$$U = 1.044\sqrt{g\lambda_b/2\pi}. \tag{10}$$

Therefore, Tab. 1 shows the reference value for λ_b, using the onset flow velocity U from Blasi et al. (2000).

According to Duncan (1981), the breaker height is proportional to the squared phase speed U and it does not depend on the slope of the forward face of the breaker:

$$a_b = 0.6 \cdot \frac{U^2}{g}. \tag{11}$$

Thus both λ_b and a_b are proportional to U^2/g for all the analyzed conditions:

$$\frac{a_b}{\lambda_b} \approx 0.1 = const. \tag{12}$$

Breaking waves are strongly asymmetric, the vertical distance from crest to trough after the breaker and the horizontal distance from the first trough to the next crest can change a lot while the ratio a_b/λ_b remains unchanged.

The breaking shape can be defined in terms of the ratio $a_b/L \sin \theta$. Duncan examines the changes in wave shape while keeping the same a_b/λ_b. In this case a trend is found:

$$L \sin \theta = \frac{a_b}{1.6}. \tag{13}$$

This gives an order of magnitude of the breaking region from toe to top.

The breaking region has been observed to have a non negligible oscillation in space and time with a regular period of 4.4 times the period of a wave with phase speed equal to the hydrofoil speed U:

$$T_b = 4.4\frac{\lambda}{U}. \tag{14}$$

It is believed that this oscillation is due to wave components produced when the onset flow is started from rest (Duncan, 1983, 2001).

The theoretical quantities defined in Eq. 10 to 14 are reported in Tab. 1 with the results from numerical simulations.

As a general comment, large differences between numerics and experiments are found in the estimate of vertical extent of the breaker $Lsin\theta$, here derived according to simple visual estimates only. The results depend not only upon the possible intrinsic weaknesses of the presented numerical approaches, but also on the uncertainty in the criterion for the breaker onset itself (see for instance Rhee and Stern

(2002)).

In Fig. 4, the time average free surface profile derived from Blasi et al. (2000) is compared to numerical results. The data from experiments (circles) show a rather wide band in which air and water are mixed (maxima and minima). Since the presence of foam implies an uncertainty in free surface location, the numerical results are presented in terms of a time average free surface value for each longitudinal position and two additional values corresponding to the maximum and minimum, analogously to the experiments. The predicted position of the first trough is downstream when compared to experimental data. The predicted first crest elevation is slightly over--predicted with O-F, F-E and F-Et approaches, while it is significantly over--predicted with O-Ft. The reason for this over--prediction with O-Ft approach is the turbulence modelling without eddy viscosity limiters. After Rhee and Stern (2002), the reason for for the wrong trough position is recognized to depend upon an inadequate pressure at the suction zone on the foil. The same type of results have been observed also in non-breaking wave cases Lupieri et al. (2012). The overestimation of the free surface could be associated to intrinsic limits of the performed simulation. The presence of breaking events takes the flow into a turbulent regime, with the consequence of enhancing the mixing at the free surface and turning on vorticity. This is a time dependent, multi scale and fully 3-D phenomenon that can lack accuracy when approached with the 2-D model used here. In particular, standard 2-D RANS simulation (continuous black line with empty squares) could reveal insufficient ability to predict properly the onset of turbulence from laminar regime. Furthermore, these numerical models are associated with an eddy viscosity production (Zhao and Armfield, 2010) that is larger than the one actually present in the experiments as estimated in recent and similar experiment (Tian et al., 2012). For this reason a simulation with a limiter for eddy viscosity has been provided (continuous blue line) with the result of a smaller breaker wave crest.

These findings support the suitability of modelling this transition flux without a turbulence model (continuous black line and red line).

Fig. 5(a) to (c) shows a waterfall of equally time spaced free surface profiles obtained from the simulations. Fig. 5(d) presents the spectral analysis of the wave elevation at $x = 2.5C$ (from the leading edge). The dominant peak is related to the breaker oscillation. The length of the time record used for the analysis is $4T_b$. The spectral analysis (see Tab. 1) confirms the periodicity as observed by Duncan (1983, 2001) for all numerical approaches. It is noteworthy that standard RANS approach can produce the sharper periodic signal since it acts as a filter for high frequency components associated to the turbulent fluctuations (Iaccarino et al., 2003), and it is therefore capable to separate them from the low frequency of the breaking phenomenon.

	λ_b/C	a_b/C	a_b/λ_b	$L\sin\theta/C$	$T_b[s]$
Eq. 10 to 14	1.78	0.18	0.1	0.11	2.81
O-F	1.38	0.12	0.087	0.03	2.53
O-Ft	1.33	0.21	0.158	0.075	2.53
F-E	2.03	0.15	0.075	0.098	2.53
F-Et	2.10	0.11	0.054	0.081	2.53

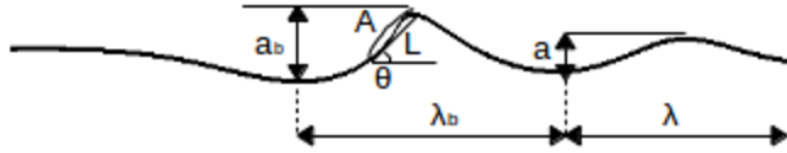Table 1: Wave shape parameters: theoretical results after Eq. 10 to 14 and numerical results.

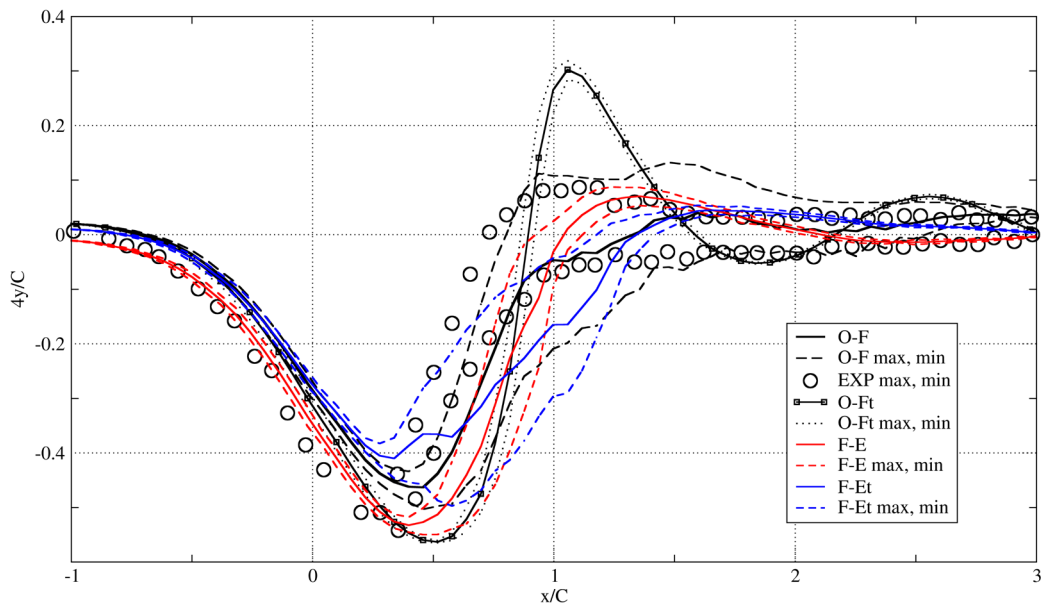Figure 3: Sketch of the surface variables of a breaking wave after Duncan (1981).

Figure 4: Time average free surface profile: black circles are experimental results by Blasi et al. (2000); solid black line is O-F without turbulence model, dashed black lines are its maxima and minima; solid black line with empty squares is O-Ft, dotted black lines are its maxima and minima; solid blue line is F-Et, dashed blue lines are its maxima and minima; solid red line is F-E, dashed red lines are its maxima and minima.
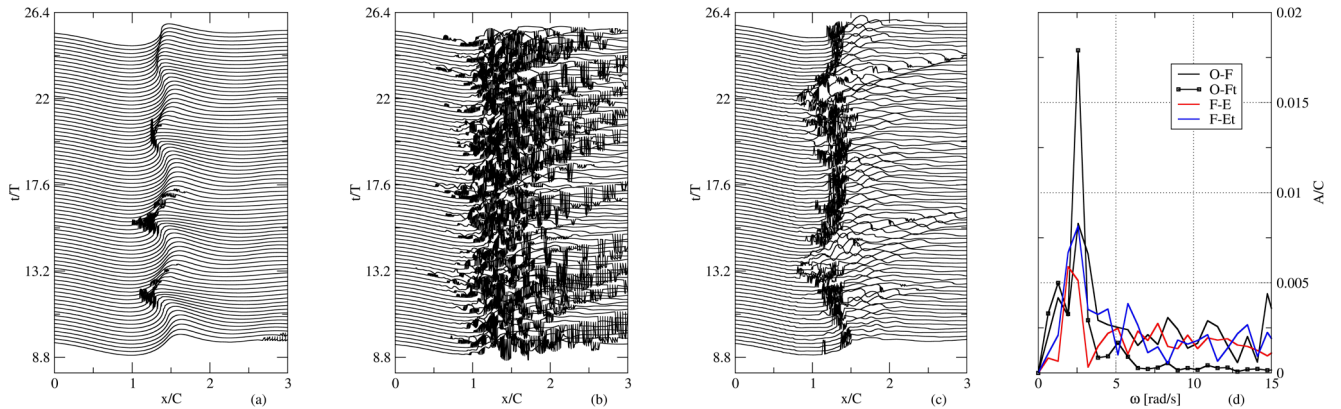
Figure 5: The cascade of free surface elevation along time as reproduced by: O-Ft (a), O-F (b) and F-E (c). The spectral analysis for all cases (d): continuous black line is O-F, continuous black line with empty squares is O-Ft, continuous blue line is F-Et, continuous red line is F-E.

6 CONCLUSIONS

Being interested in the ship resistance in the presence of breaking events, the case of a laboratory experiment has been investigated with 2-D numerical simulations. The case considers a foil underneath the free surface, positioned at a fixed distance, and exposed to a controlled flux. The unperturbed flow lays in a laminar regime except where the breaking event occurs. The breaking produces a mixture of air and water at the free surface interface and this could justify the need for turbulence modelling. The goal of this study is to resolve the RANS equations to extract information related to breaking wave events.

The standard RANS approach is inadequate in the reproduction of the surface elevation and in the detection of the first through position when compared to simulations without turbulence modelling. On the contrary, the periodicity of the breaking event predicted by theory is more expressed in RANS approach.

The reasons for the partial unsuitability of RANS approach in the selected case have been discussed exhaustively and lead the authors to consider different paths for high accuracy simulations of wave resistance on ship hulls. In particular, the high level of eddy viscosity produced by the turbulence model adopted here should be limited. This could be done with a different formulation of the turbulence production term, as sometimes done in external aerodynamic flows with high streamline curvature. A radically different approach could be Large Eddy Simulations or the promising Detached Eddy Simulation technique, laying between RANS and LES, with consequent increase in computing time and data storage.

7 ACKNOWLEDGEMENTS

References

Blasi, P. D., Romano, G. and Felice, F. D. (2000), `Experimental study of breaking wave flow field past a submerged hydrofoil by ldv', *Int. Journal of Offshore and Polar Engineering* **4**(10).

Dong, R., Katz, J. and Huang, T. (1997), `On the structure of bow waves on a ship model', *J. Fluid Mech* **347**, 77--115.

Duncan, J. (1981), `An experimental investigation of breaking waves produced by a towedhydrofoil', *Proc. R. Soc. Lond.* **A 377**, 331--348.

Duncan, J. (1983), `The breaking and non-breaking wave resistance of a two-dimensional hydrofoil', *J. Fluid Mech.* **126**, 507--520.

Duncan, J. (2001), `Spilling breakers', *Annu. Rev. Fluid Mech.* (33), 519--547.

foam-extend project. http://www.extend-project.de/, accessed 18/March/2015 (2014).

Gomez, P., Hernández, J. and López, J. (2005), `On the reinitialization procedure in a narrow--band locally refined level set method for interfacial flows', *Int. Journal for Numerical Methods in Engineering* **63**, 1478--1512.

Hartmann, D., Meinke, M. and Schröde, W. (2008), `Differential equation based constrained reinitialization for level set methods', *J. Comput. Phys.* **22**, 6821--6845.

Hirt, C. and Nichols, B. (1981), `Volume of fluid (vof) method for the dynamics of free boundaries', *J. Comput. Phys* **39**, 201--225.

Iaccarino, G., Ooi, A., Durbin, P. and Behnia, M. (2003), `Reynolds averaged simulation of unsteady separated flow', *Int. Journal of Heat and Fluid Flow* **24**, 147--156.

Lupieri, G., Puppo, N. D., Morgut, M., Contento, G., Nobile, E., Genuzio, H. and Lavini, G. (2012), Openship project - numerical predictions of ship and propeller hydrodynamics by opensource cfd: Results from preliminary benchmark tests, *in* `Proceedings from NAV 2012, 17th International Conference on Ships and Shipping Research and Advancing with Composite 2012 Symposium'.

Menter, F. (1994), `Two-equation eddy-viscosity turbulence models for enigineering applications', *AIAA Journal* (8), 1598--1605.

Muscari, R. and Mascio, A. D. (2004), `Numerical modeling of breaking waves generated by a ship's hull', *Journal of Marine Science and Technology* **9**, 158--179.

OpenFOAM (2012), *OpenFOAM User Guide, OpenCFD Ltd* .

Osher, S. and Sethian, J. (1988), `Fronts propagating with curvature dependent speed: Algorithms based on hamilton-jacobi formulations', *J. Comput. Phys.* **79**, 12--49.

Rhee, S. and Stern, F. (2002), `Rans model for spilling breaking waves', *Journal of Fluids Engineering,ASME* **124**, 424--432.

Roth, G., Mascenik, D. and Katz, J. (1999), `Measurements of the flow structure and turbulence within a ship bow wave. physics of fluids', pp. 3512--3523.

Rusche, H. (2002), `Computational fluid dynamics of dispersed two - phase flows at high phase fractions'.

Sun, Y. and Beckermann, C. (2007), `Sharp interface tracking using the phase--field equations', *J. Comput. Phys.* **220**, 626--653.

Tian, Z., Perlin, M. and Choi, W. (2012), `An eddy viscosity model for two-dimensional breaking waves and its validation with laboratory experiments', *Physics of Fluids* **24**(036601).

Vukčević, V., Jasak, H. and Malenica, . (2015), Solution and domain decomposition model for naval hydrodynamics: Rans and potential flow coupling, *in* `VI International Conference on Computational Methods in Marine Engineering (MARINE 2015) - in press'.

Zhao, Q. and Armfield, S. (2010), `Recent advances in turbulence modelling for unsteady breaking waves', *Book chapter in Advances in Coastal and Ocean Engineering* **11**, 605--640.